

Article

Catalytic Behavior of Lipase Immobilized onto Congo Red and PEG-Decorated Particles

Rubens A. Silva, Ana M. Carmona-Ribeiro and Denise F. S. Petri *

Instituto de Química, Universidade de São Paulo, Av. Prof. Lineu Prestes 748, São Paulo 05508-000, SP, Brazil; E-Mails: rubens.silva@usp.br (R.A.S.); amcr@usp.br (A.M.C.-R.)

* Author to whom correspondence should be addressed; E-Mail: dfsp@iq.usp.br;
Tel.: +55-11-3091-3831; Fax: +55-11-3815-7759.

Received: 4 May 2014; in revised form: 20 June 2014 / Accepted: 20 June 2014 /

Published: 24 June 2014

Abstract: Poly(ethylene glycol) (PEG)-decorated polystyrene (PS) nanoparticles with mean hydrodynamic diameter (D) and zeta-potential (ζ) of (286 ± 15) nm and (-50 ± 5) mV, respectively, were modified by the adsorption of Congo red (CR). The PS/PEG/CR particles presented D and ζ values of (290 ± 19) nm and (-36 ± 5) mV, respectively. The adsorption of lipase onto PS/PEG or PS/PEG/CR particles at (24 ± 1) °C and pH 7 changed the mean D value to (380 ± 20) and (405 ± 11) nm, respectively, and ζ value to (-32 ± 4) mV and (-25 ± 2) mV, respectively. The kinetic parameters of the hydrolysis of *p*-nitrophenyl butyrate were determined for free lipase, lipase immobilized onto PS/PEG and PS/PEG/CR particles. Lipase on PS/PEG/CR presented the largest Michaelis-Menten constant (K_M), but also the highest V_{\max} and k_{cat} values. Moreover, it could be recycled seven times, losing a maximum 10% or 30% of the original enzymatic activity at 40 °C or 25 °C, respectively. Although lipases immobilized onto PS/PEG particles presented the smallest K_M values, the reactions were comparatively the slowest and recycling was not possible. Hydrolysis reactions performed in the temperature range of 25 °C to 60 °C with free lipases and lipases immobilized onto PS/PEG/CR particles presented an optimal temperature at 40 °C. At 60 °C free lipases and lipases immobilized onto PS/PEG/CR presented ~80% and ~50% of the activity measured at 40 °C, indicating good thermal stability. Bioconjugation effects between CR and lipase were evidenced by circular dichroism spectroscopy and spectrophotometry. CR molecules mediate the open state conformation of the lipase lid and favor the substrate approaching.

Keywords: lipase; poly(ethylene glycol); Congo red; kinetic parameters; bioconjugation

1. Introduction

Immobilized enzymes are “green” catalysts for many reactions of industrial interest. They can be advantageous compared to free enzymes because: (i) immobilization improves their stability; (ii) subsequent reuse is possible; (iii) inhibition by products or sub-products is avoided; (iv) optimum pHs and temperatures might shift to more convenient values. However, the immobilized enzymes must maintain their active sites in a suitable orientation in order to retain their catalytic properties and the costs related to the support and to the immobilization process should be as low as possible [1].

Lipases are probably the most used enzymes in hydrolysis, esterification, acidolysis and alcoholysis reactions. Some of the reasons for this are their low cost, compared to other enzymes, high stability in organic media or emulsions or under extreme reactions conditions (pH, ionic strength and temperature), broad substrate specificity and the catalysis of regio- and enantioselective reactions [2]. Lipases are hydrolases composed of a core of predominantly parallel β strands surrounded by α helices [3]. The active site of lipases is formed by a catalytic triad consisting of the amino acids serine, histidine and aspartic acid/glutamic acid [4], which is covered by a lid or flap composed of an amphiphilic α -helix peptide sequence. In the presence of hydrophobic substrates, the lid is displaced and the active site is exposed. Lipases have been successfully immobilized in a large variety of surfaces by different techniques. The literature is plenty of excellent reviews on this subject, as for instance, references [1,5–9]. In a general form, enzymes can be physically or chemically attached to surfaces, entrapped in networks or cross-linked in aggregates (CLEA) [9]. Hydrophobic carriers favor the physical adsorption of lipases by means of van der Waals interactions and entropic gain due to water molecule release, whereas H bonding or ion pair formation drives the adsorption onto hydrophilic supports. Although physically immobilized lipases might be partially leached out under industrial conditions their preparation is usually simple, cheap and the support can be reused. Hydrophobic surfaces tend to promote the interfacial activation of lipases, which is crucial for their catalytic efficiency [10–14]. Nevertheless, Ye and coworkers observed that although the adsorption of lipase onto bare polystyrene (PS), a hydrophobic polymer, was more pronounced than onto hydrophilically modified PS, the activity retention of immobilized lipases was higher on the hydrophilic surfaces [15].

Creating novel surfaces which combine chemical functionality and large surface areas, opens the possibility to learn about the behavior of biomolecules immobilized on them. In the present paper spherical nanoparticles with different functionalities were prepared to serve as supports for the immobilization of lipases. PS particles decorated with hydrophilic PEG molecules and hydrophobic Congo red (CR) molecules were synthesized. The catalytic properties of lipases immobilized onto hydrophilic and hydrophobic surfaces were compared with those determined for free lipases. The role played by PEG and Congo red molecules on the catalytic properties of immobilized lipase was discussed. Previous studies showed that PS/PEG particles are adequate supports for the immobilization of bovine serum albumin (BSA), concanavalin A (Con A) or cholesterol oxidase (ChOx) [16–18]. However, in the case of immobilized ChOx onto PS/PEG, no enzymatic activity could be observed,

probably due to ChOx denaturation, unfavorable orientation or low accessibility of the substrate (cholesterol) to the active site positioned in the hydrated PEG environment [18]. The modification of PS/PEG particles by the adsorption of CR molecules, which have amphiphilic character and shows ability to bind to PEG [19] and polypeptides [20], overcomes the unfavorable situation. In the case of ChOx, bioconjugation effects between CR and ChOx or cholesterol mediated not only the immobilization but also the activation of ChOx immobilized onto PS/PEG/CR particles [18]. In the present work the immobilization of *Candida rugosa* lipases onto hydrophilic PS/PEG or hydrophobic PS/PEG/CR particles was investigated by adsorption isotherms, light scattering and zeta-potential (ζ) measurements. Although the adsorption of lipases onto hydrophobic surfaces tends to be more favorable than onto hydrophilic supports, the dependence of activity retention on the surface hydrophobicity seems controversial [15]. *C. rugosa* lipase was chosen because it is one of the most frequently used enzymes in biotechnological processes. It can be produced in large scale with good quality. *C. rugosa* lipase is composed of a mixture of isoenzymes (Lip1–Lip5) with specific catalytic properties, being Lip1 the mostly found isoenzyme in the commercial samples. In spite of the fact that the relationship between the fermentation conditions, isoenzymes structures and biocatalytical performances might be rather complex, *C. rugosa* lipases show large potential for biotechnological applications [19]. The kinetic parameters determined at 25 °C for the hydrolysis of *p*-nitrophenyl butyrate (*p*-NPB) catalyzed by free lipases and for lipases immobilized onto PS/PEG/CR particles were comparable, and they were superior to those determined for lipases immobilized onto PS/PEG particles. Bioconjugation effects between CR and lipases or *p*-NPB were evaluated by means of circular dichroism and spectrophotometry. Thermal stability of immobilized lipases was compared to that of free lipases.

2. Results and Discussion

2.1. Characteristics of PS/PEG and PS/PEG/CR Particles

Dispersions of PS/PEG and PS/PEG/CR presented size distribution histograms, as shown in Figure 1a,b, respectively. Table 1 presents the mean diameter (D), polydispersity (P) and zeta-potential (ζ) values determined from triplicates for PS/PEG and PS/PEG/CR particles. The mean D values determined by DLS corroborated with the typical particle sizes observed by scanning electron micrographies (insets in Figure 1a,b). One should note that the preparation of PS/PEG/CR particles corresponds to the adsorption plateau of $\sim 5.0 \pm 0.2 \mu\text{mol}\cdot\text{g}^{-1}$, as described elsewhere [18]. After CR adsorption the average particle size didn't increase significantly, but the P values increased 20%. A small contribution of particles with $D \sim 100$ nm appeared (Figure 1b), which might be due to partial aggregation induced by the CR adsorption.

The ζ -potential of (-50 ± 5) mV observed for PS/PEG particles is a consequence of the dissociation of sulfate groups (from the polymerization initiator potassium persulfate) at the interface, which has ionic strength different from that of the bulk due to the electric double-layer. After CR adsorption the ζ -potential changed to (-36 ± 5) mV. Interactions between partially protonated CR amine groups and sulfate groups or ethylene glycol oligomers on the PS/PEG particles drive the adsorption of CR onto PS/PEG particles, causing the reduction in the ζ -potential values.

Figure 1. Particle size distribution histograms determined for (a) PS/PEG and (b) PS/PEG/CR particles. The insets correspond to SEM images taken for dried dispersions.

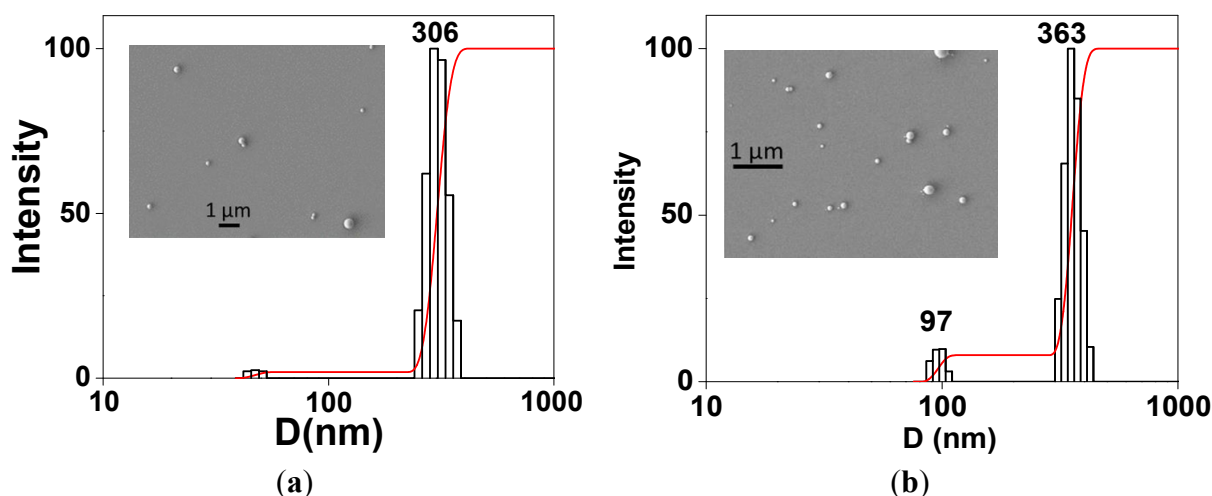


Table 1. Mean diameter (D), polydispersity (P) and zeta-potential (ζ) values determined for PS/PEG and PS/PEG/CR particles before and after lipase adsorption at (a) $Q_{\text{lipase}} = (85 \pm 3) \text{ nmol}\cdot\text{mg}^{-1}$ and (b) $Q_{\text{lipase}} = (105 \pm 5) \text{ nmol}\cdot\text{mg}^{-1}$.

| | D (nm) | ζ (mV) | P |
|---------------------------------|--------------|---------------|-----------------|
| PS/PEG | 286 ± 15 | $-(50 \pm 5)$ | 0.17 ± 0.01 |
| PS/PEG/CR | 290 ± 19 | $-(36 \pm 5)$ | 0.21 ± 0.02 |
| PS/PEG/lipase ^(a) | 380 ± 20 | $-(32 \pm 4)$ | 0.20 ± 0.03 |
| PS/PEG/CR/lipase ^(b) | 405 ± 11 | $-(25 \pm 2)$ | 0.27 ± 0.05 |

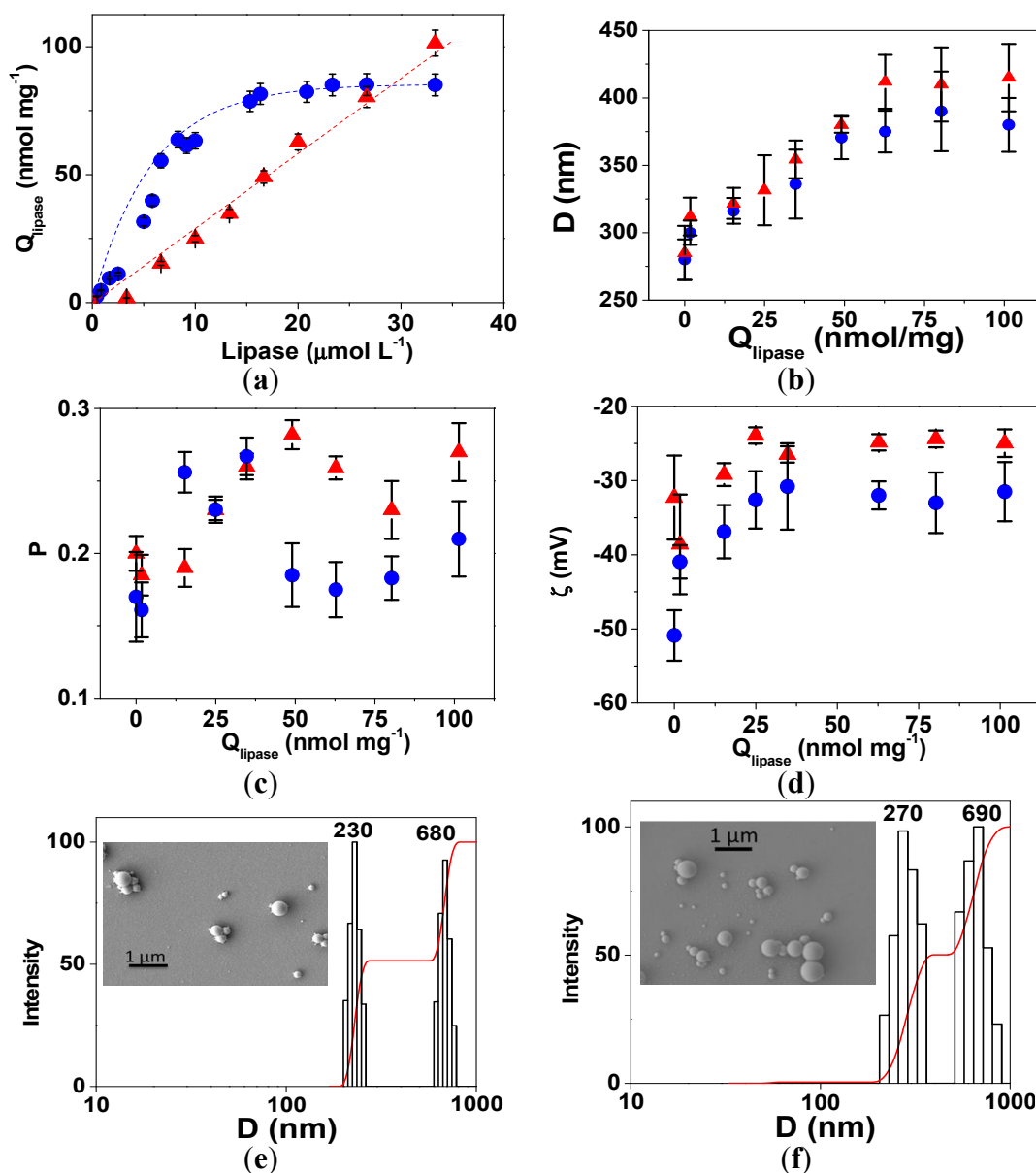
For the sake of comparison the synthesis of PS particles was carried out using $\text{K}_2\text{S}_2\text{O}_8$ as initiator, but instead of Tween-20 as emulsifier, sodium dodecyl sulfate (SDS) was employed; these particles were coded as PSS. The particles presented mean diameter of (342 ± 20) nm and zeta potential value of (-64 ± 2) mV. The PSS and PS/PEG particles carry sulfate charges on the surface, but only PS/PEG particles are decorated with ethylene glycol oligomers. The adsorption experiments of CR onto PSS particles were performed in the same way as those for CR onto PS/PEG particles. However, the amount of CR adsorbed onto PSS was only 5% of that of CR onto PS/PEG particles. The main reason for this is the electrostatic repulsion between sulfate groups on PSS particles and CR sulfonate groups. These findings show that the interaction between ethylene glycol oligomers on the PS/PEG particles is crucial for the CR adsorption. The use of cationic surfactant, namely, cetyltrimethylammonium bromide (CTAB), for the synthesis of PS particles led to colloidal instability and partial aggregation already before CR adsorption experiments.

2.2. Adsorption Behavior of Lipase onto PS/PEG or PS/PEG/CR Particles

The adsorption isotherms of lipase onto PS/PEG or PS/PEG/CR particles at (24 ± 1) °C and pH 7 are presented in Figure 2a. The adsorbed amount of lipase (Q_{lipase}) onto PS/PEG particles increased linearly with the lipase concentration until the adsorption plateau at $(85 \pm 3) \text{ nmol}\cdot\text{mg}^{-1}$ was achieved. On the other hand, Q_{lipase} onto PS/PEG/CR particles increased linearly and continuously with the lipase

concentration. For lipase concentrations smaller than $27 \mu\text{mol}\cdot\text{L}^{-1}$ the Q_{lipase} values onto PS/PEG were higher than those determined for lipase onto PS/PEG/CR particles. However, for lipase bulk concentrations larger than $27 \mu\text{mol}\cdot\text{L}^{-1}$ the opposite trend is observed. The largest Q_{lipase} value determined for lipase onto PS/PEG/CR particles was $(105 \pm 5) \text{ nmol}\cdot\text{mg}^{-1}$. The experimental isotherms were not fitted to the theoretical models because in both cases the adsorption is irreversible (less than 10% desorption) and the surfaces are not chemically homogeneous due to the presence of sulfate, ethylene glycol oligomers and CR functional groups.

Figure 2. (a) Adsorption isotherms determined at $(24 \pm 1) ^\circ\text{C}$ and pH 7.0 for lipase onto PS/PEG (blue circles) and PS/PEG/CR particles (red triangles). The lines are guides for the eyes. (b) Mean D , (c) PD and (d) ζ -potential values determined for PS/PEG or PS/PEG/CR particles after lipase adsorption as a function of Q_{lipase} . Particle size distribution histograms and SEM images (insets) obtained for (e) PS/PEG and (f) PS/PEG/CR particles after lipase adsorption, $Q_{\text{lipase}} = 85 \pm 3 \text{ nmol}\cdot\text{mg}^{-1}$ and $Q_{\text{lipase}} = 105 \pm 5 \text{ nmol}\cdot\text{mg}^{-1}$, respectively. Each point is the average of triplicates \pm SD.



The mean D values determined for PS/PEG or PS/PEG/CR particles after lipase adsorption increased with Q_{lipase} (Figure 2b) up to D values of 405 ± 11 nm and 380 ± 20 nm, corresponding to plateau value ($Q_{\text{lipase}} = 85 \pm 3$ nmol·mg⁻¹) for PS/PEG particles, and to the highest value ($Q_{\text{lipase}} = 105 \pm 5$ nmol·mg⁻¹) for PS/PEG/CR particles, respectively, as presented in Table 1. For both systems the PD values fluctuated from 0.15 to 0.30 (Figure 2c), probably due to the bimodal size distribution evidenced by the histograms in Figure 2e,f, which indicate one population has the typical size of isolated particles and the second population has mean size corresponding to doublets, as evidenced by scanning electron micrographies (insets in Figure 2e,f).

Upon increasing Q_{lipase} , the ζ -potential values (in modulus) decreased up to constant values of (-32 ± 4) mV and (-25 ± 2) mV, for PS/PEG and PS/PEG/CR, respectively (Figure 2d). The adsorption of lipases on PS/PEG surfaces might be driven by electrostatic interaction between lipase positively charged residues and sulfate groups on the PS/PEG particles. Although at pH 7 the lipase net charge is negative because its isoelectric point (pI) is 4.5 [21], there are patches of positively charged residues that are able to bind to the negatively charged surface, reducing the module of ζ -potential values. Similar behavior was observed for cholesterol oxidase onto PS/PEG particles [18] or bovine serum albumin (BSA) onto polyanions [22,23]. In the case of PS/PEG/CR not only the electrostatic interaction but also the hydrophobic interactions drive the immobilization of lipases and reduction of the modulus of ζ -potential values. Therefore, the reduction in ζ -potential modulus values decreases the electrostatic repulsion among the particles and favors the partial formation of doublets by van der Waals attraction.

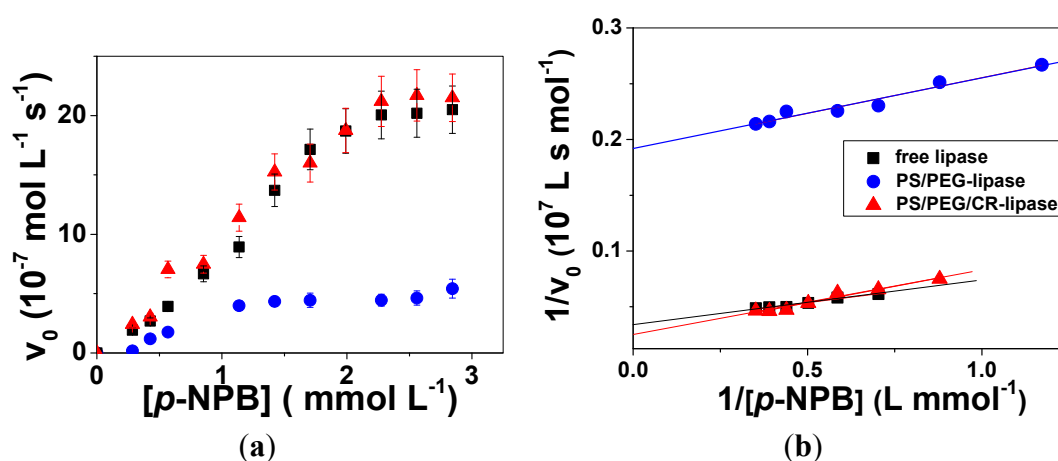
One important aspect regards the monomeric or dimeric state of immobilized lipases. This issue was treated in details by the group of Guisan and Fernández-Lafuente [24–28]. At moderate lipase concentrations the dimerization takes place in solution and at the support due to interactions between the hydrophobic areas of the lipase surface that surround the active site of the open form of two lipase molecules. However, in the presence of detergent (0.1% v/v Triton X-100) the dimerization is reduced. The main consequence is that the catalytic properties of lipases immobilized as dimers differ from those of immobilized as monomers [24]. The increase in the mean D values after lipase adsorption on the order of 100 nm shown in Table 1 is mainly due to partial particles aggregation and cannot be discussed in terms of adsorption of lipases monomers or dimers. One strategy to evaluate if lipases were immobilized as monomers or dimers onto PS/PEG or PS/PEG/CR particles is to use flat Si/SiO₂ or CR covered Si/SiO₂ wafers to represent the particles and to determine the thickness of adsorbed lipases by means of ellipsometry. Ellipsometry is an optical technique based on the changes of the light polarization state after reflecting from a planar homogeneous isotropic surface, which allows determining the thickness (>0.1 nm) of very thin films, distinguishing monolayers, bilayers or multilayers [29,30]. One should notice that a flat and homogeneous covalently bound PEG layer on a planar surface is not trivially formed. On the other hand, Si/SiO₂ wafers are very hydrophilic surfaces, as PS/PEG particles, and are convenient surfaces for ellipsometry because they are very flat and homogeneous. Si/SiO₂ wafers or CR covered Si/SiO₂ wafers interacted with solutions of lipase at $16.6 \mu\text{mol L}^{-1}$ (1.0 g/L) and $33 \mu\text{mol L}^{-1}$ (2.0 g/L) in the absence and in the presence of TritonX-100 at 0.2 mM, under equilibrium conditions at (24 ± 1) °C. The ellipsometric data revealed that regardless the lipase concentration and the presence of Triton X-100, the mean thickness values of adsorbed lipase layer onto Si/SiO₂ and CR covered Si/SiO₂ wafers were (1.5 ± 0.2) nm and (1.7 ± 0.2) nm,

respectively. Considering the radius of gyration of lipase in water as 1.67 nm [31], the thickness values determined for immobilized lipases onto Si/SiO₂ and CR covered Si/SiO₂ wafers were attributed to the formation of lipases monolayer. Thus, if large aggregates were present on the surface, they would yield layers much thicker than those observed for lipases immobilized onto Si/SiO₂ or CR covered Si/SiO₂ wafers.

2.3. Enzymatic Activity of Free and Adsorbed Lipase

The enzymatic activity of free and adsorbed lipase onto PS/PEG or PS/PEG/CR particles was monitored by the formation of *p*-NP as a function of time. The dependence of the initial rates of *p*-NP formation on the concentration of *p*-NPB is presented in Figure 3a. For the enzymatic assays with lipase adsorbed onto PS/PEG and PS/PEG/CR particles the highest Q_{lipase} values, namely, $Q_{\text{lipase}} = (85 \pm 3) \text{ nmol}\cdot\text{mg}^{-1}$ and $(105 \pm 5) \text{ nmol}\cdot\text{mg}^{-1}$, respectively, were employed. For the determination of enzymatic activity of free lipase, the concentration was set at $0.4 \mu\text{mol}\cdot\text{L}^{-1}$, because it corresponds to the bulk concentration used to achieve the above mentioned Q_{lipase} values (see Experimental Section for details). The experimental data were fitted with Lineweaver-Burk plots, as shown in Figure 3b. The fitting parameters maximum rate (V_{max}), Michaelis constant (K_M), turnover number (k_{cat}) and catalytic efficiency (ϵ) are shown in Table 2. The k_{cat} values were determined dividing the V_{max} values by the enzyme bulk concentration ($0.4 \mu\text{mol}\cdot\text{L}^{-1}$). The ϵ values were calculated dividing k_{cat} by K_M values.

Figure 3. (a) Initial rates determined for the hydrolysis of *p*-NPB catalyzed by free lipase (black squares) at $0.4 \times 10^{-6} \text{ mol/L}$ and lipase immobilized onto PS/PEG (blue circles, $Q_{\text{lipase}} = 85 \pm 3 \text{ nmol}\cdot\text{mg}^{-1}$) or onto PS/PEG/CR (red triangles, $Q_{\text{lipase}} = 105 \pm 5 \text{ nmol}\cdot\text{mg}^{-1}$) as a function of *p*-NPB concentration. Each point is the average of triplicates \pm SD. (b) Lineweaver-Burk fitting curves for free lipase (black squares) and lipase immobilized onto PS/PEG (blue circles) and PS/PEG/CR (red triangles).



A comparison among the kinetic parameters determined for the reactions in the presence of free lipases and lipases immobilized onto PS/PEG particles and PS/PEG/CR particles reveals interesting interfacial effects. The smallest K_M values were observed for lipases immobilized onto PS/PEG particles, indicating larger affinity for *p*-NPB than free lipase or lipase immobilized onto PS/PEG/CR. The highly hydrated PEG oligomers provided an environment which was more favorable than the

others. This finding is in agreement with results reported for the enzymatic activity of lipases immobilized onto hydrophobic and hydrophilic polymeric supports [15]. On the other hand, the V_{\max} values determined for lipase onto PS/PEG showed slower enzymatic activity compared to those of free lipases or lipases immobilized onto PS/PEG/CR. This effect is probably due to the hydrophilic nature of PS/PEG particles surfaces, which doesn't help to promote the lipase open-state conformation. A similar effect was observed for cholesterol oxidases (ChOx), which adsorbed onto PS/PEG particles but presented no enzymatic activity [18]. In solution the effect of PEG on the enzyme conformation and activity seems to depend on the enzyme type and on PEG molecular weight, for instance, PEG 400 changed the conformation of chymotrypsin, retarding the degradation of insulin [32], the enzymatic activity of hexokinase increased 6% in the presence of PEG 400 and decreased in the range 14%–7% in the presence of PEG 1500 and PEG 4000, respectively, due to aggregation [33], PEG 400 or 4000 presented no interaction with glucose-6-phosphate dehydrogenase (G-6-PDH), but favorable interactions were observed between PEG and the co-enzyme NADP^+ , which increased the enzymatic activity in 20% [34]. Comparing the activities in the presence of PEG 200, PEG 8000 or PEG 12000, the enzymatic activity of lipase increased 161% in the presence of PEG 12000 [35]. In the case of PS/PEG particles the PEG chains stem from the surfactant (Tween 20) and have in average only five repeating units, rendering ~ 200 g/mol. The literature studies cited above indicate that PEG chains are not inert with respect to enzyme conformation; specific interaction and hydration effects might induce changes in chain conformation and orientation.

Table 2. Kinetic parameters determined for the hydrolysis of *p*-NPB catalyzed by free lipase at $0.4 \times 10^{-6} \text{ mol}\cdot\text{L}^{-1}$ and lipase immobilized onto PS/PEG ($Q_{\text{lipase}} = 85 \pm 3 \text{ nmol}\cdot\text{mg}^{-1}$) or onto PS/PEG/CR ($Q_{\text{lipase}} = 105 \pm 5 \text{ nmol}\cdot\text{mg}^{-1}$). V_{\max} , K_M , k_{cat} and ϵ stand for maximal rate, Michaelis constant, turnover number and catalytic efficiency, respectively.

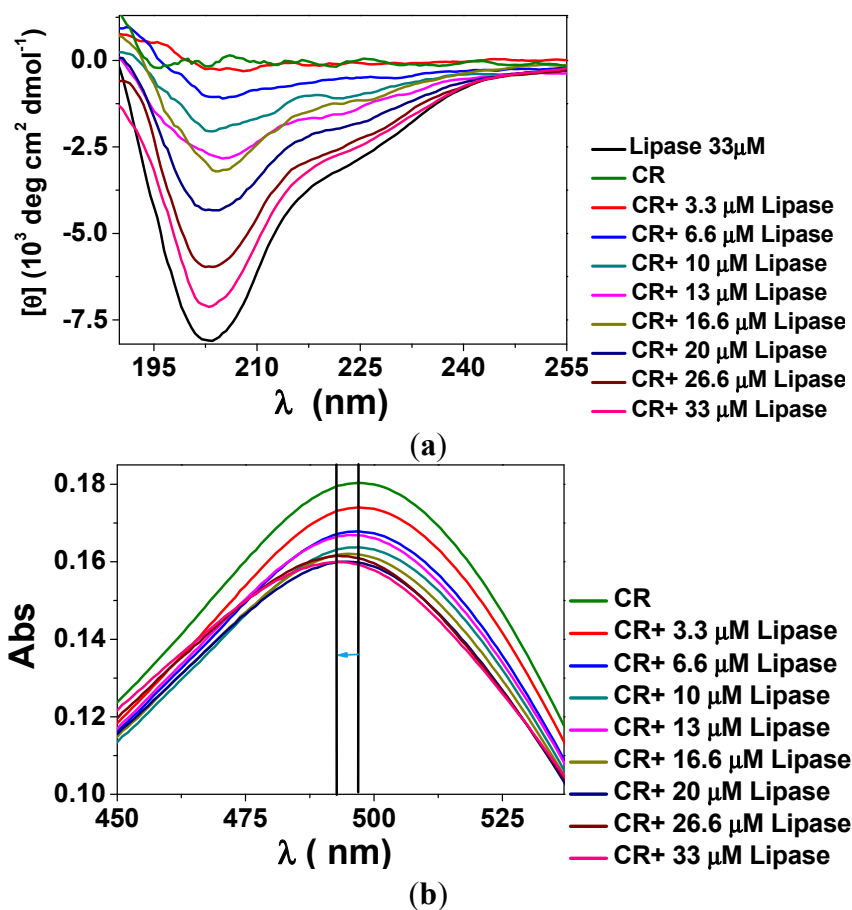
| System | V_{\max} ($10^{-7} \text{ mol}\cdot\text{L}^{-1}\cdot\text{s}^{-1}$) | K_M ($10^{-3} \text{ mol}\cdot\text{L}^{-1}$) | k_{cat} (s^{-1}) | ϵ ($\text{L s}^{-1}\cdot\text{mol}^{-1}$) |
|------------------|---|--|---|---|
| Free lipase | 30.3 ± 0.5 | 1.25 ± 0.08 | 7.5 ± 0.8 | 6000 ± 691 |
| PS/PEG/CR-Lipase | 46 ± 1 | 2.9 ± 0.5 | 11 ± 1 | 3958 ± 344 |
| PS/PEG-Lipase | 5.2 ± 0.5 | 0.32 ± 0.04 | 1.3 ± 0.1 | 4053 ± 678 |

The K_M value found for free lipase was $1.25 \pm 0.08 \text{ mmol}\cdot\text{L}^{-1}$ (Table 2), similar to the ones determined for chemically immobilized *Candida rugosa* lipase onto amino-terminated polypropylene [36] or for *Rhodotorula Glutinis* lipase in the hydrolysis of *p*-NPB [37]. Lipase immobilized onto PS/PEG/CR particles presented K_M value of $2.9 \pm 0.5 \text{ mmol}\cdot\text{L}^{-1}$, indicating that the affinity for *p*-NPB decreased in comparison to that in solution or onto PS/PEG particles. However, the largest V_{\max} and k_{cat} values were achieved for lipases adsorbed onto PS/PEG/CR particles. These findings indicate that although the affinity between lipase and *p*-NPB was not the largest among the three systems, the presence of CR molecules on the polymer particles turned the environment more hydrophobic, which is suitable for the interfacial activation of lipases [38]. The latter requires: (i) lid opening with consequent conformational changes and (ii) orientation of substrate at the interface. The amphiphilic character of CR molecules due to the hydrophobic aromatic rings and amine and sulphonate polar groups seems to favor the interaction between lipase active site and *p*-NPB, keeping the hydration at a reasonable level. The enzymatic activity of physically bound lipases tend to be similar or even larger

than that of free lipase, when the supports are partially hydrophobic but carry hydrophilic groups that keep the hydration level necessary to the hydrolysis reactions. For instance, lipase immobilized onto cellulose ester films exhibited activity higher than that of free lipase and could be recycled three times and stored for one month keeping the activity at a reasonable level [10]. The interaction between the hydrophobic moieties of cellulose esters and the lid helped to keep the open-state conformation, while the hydroxyl groups of glycosidic rings interacted with water molecules. Other supports with similar behavior are zirconia nanoparticles modified by surfactant molecules [11], cyclodextrin-based carbonate nanosponge [12], ethylene–vinyl alcohol polymer functionalized with acyl chlorides [13], multiwalled carbon nanotubes modified by amino-cyclodextrin [14].

In order to gain insight about the interactions between CR molecules and lipase, circular dichroism (CD) and electronic spectra were taken for mixtures of CR at $8.0 \mu\text{mol}\cdot\text{L}^{-1}$ and lipase at increasing concentration from $3 \mu\text{mol}\cdot\text{L}^{-1}$ to $33 \mu\text{mol}\cdot\text{L}^{-1}$, as shown in Figure 4a,b, respectively. CR presented no CD signal in the range between 190 nm and 260 nm. CD spectrum obtained for pure lipase corresponds to $\sim 22\%$ of helical structure, which is typical for lipases [39], with minimum at ~ 204 nm and broad shoulder in the range of 220 nm to 225 nm (Figure 4a). Such typical features could be observed in the mixtures of lipase at concentrations larger than $13 \mu\text{mol}\cdot\text{L}^{-1}$ and CR, indicating that CR molecules do not promote lipase conformational changes. For lipase concentration smaller than $13 \mu\text{mol}\cdot\text{L}^{-1}$ the CD signal became too weak.

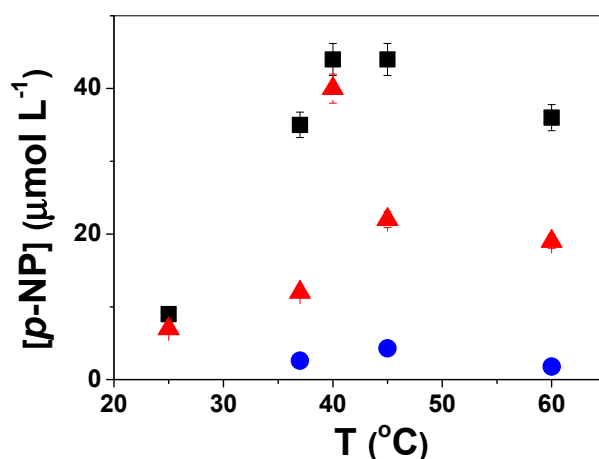
Figure 4. (a) Circular dichroism (CD) and (b) electronic spectra obtained for mixtures of CR at $8.0 \mu\text{mol}\cdot\text{L}^{-1}$ and lipase at increasing concentration from $3.3 \mu\text{mol}\cdot\text{L}^{-1}$ to $33 \mu\text{mol}\cdot\text{L}^{-1}$.



The electronic spectra obtained for pure CR at $8.0 \mu\text{mol}\cdot\text{L}^{-1}$ (Figure 4b) presented two $\pi \rightarrow \pi^*$ transitions, one at 497 nm (the strongest) and another at 350 nm (not shown), and low-intensity $n \rightarrow \pi^*$ transition associated to the azo group [40]. As lipase was added to the system a blue shift (hypsochromic effect) in the maximum was detected. At the highest lipase concentration ($33 \mu\text{mol}\cdot\text{L}^{-1}$) the shift was 5 nm. Such hypsochromic effect is generally due to increase of medium polarity and has been already observed for mixtures of CR and cholesterol oxidase [18]. Thus, the blue shift observed in Figure 4b might indicate bioconjugation mediated by H bonding between CR amine groups and lipase polar residues. Electronic spectra obtained for mixtures of CR at $8.0 \mu\text{mol}\cdot\text{L}^{-1}$ and *p*-NPB in the concentration range between $0.3 \text{ mmol}\cdot\text{L}^{-1}$ and $3.0 \text{ mmol}\cdot\text{L}^{-1}$ showed no shift regarding the absorption band at 497 nm, indicating no bioconjugation effect between CR and *p*-NPB.

The thermal stability of free and immobilized lipases was investigated by monitoring the formation of *p*-NP after 20 min hydrolysis in the temperature range from 25 °C to 60 °C, as shown in Figure 5. No shift of optimal temperature was observed for lipases immobilized onto PS/PEG/CR particles (red triangles) in comparison to free lipases (black squares), since for both systems the highest hydrolytic activity was observed at 40 °C. At 60 °C free lipase and lipase immobilized onto PS/PEG/CR presented ~80% and ~50% of the activity measured at 40 °C. Lipases immobilized onto chitosan presented similar behavior [41]. Regardless the temperature, the activity observed for lipases immobilized onto PS/PEG particles was very low in comparison to those determined for free lipase or lipases immobilized onto PS/PEG/CR particles.

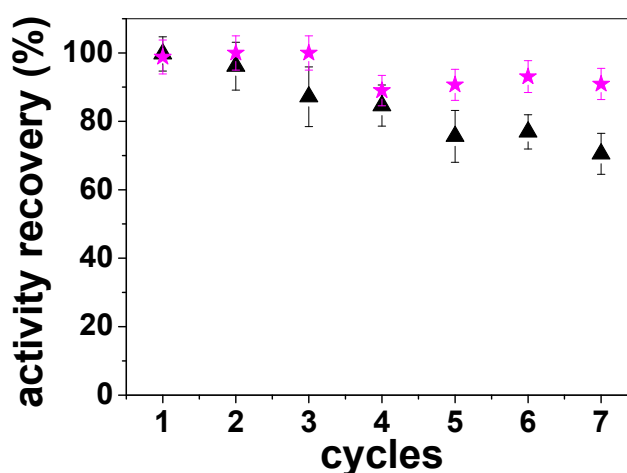
Figure 5. Concentration of *p*-NP formed from the hydrolysis of *p*-NPB catalyzed by free lipases (black squares), lipases immobilized onto PS/PEG/CR (red triangles, $Q_{\text{lipase}} = 105 \pm 5 \text{ nmol}\cdot\text{mg}^{-1}$) and PS/PEG (blue circles, $Q_{\text{lipase}} = 85 \pm 3 \text{ nmol}\cdot\text{mg}^{-1}$) particles at 25 °C, 37 °C, 40 °C, 45 °C and 60 °C. Each point is the average of triplicates \pm SD.



Lipase immobilized onto PS/PEG/CR particles ($Q_{\text{lipase}} = 105 \pm 5 \text{ nmol}\cdot\text{mg}^{-1}$) could be recycled consecutively seven times. Figure 6 presents the activity recovery (%), which is the activity of immobilized lipase compared to that of total starting activity of free lipase [9], determined at 25 °C (black triangle) and 40 °C (pink star). The enzymatic activities of free and immobilized lipase were comparable in the first use at both temperatures. Then the activity recovery decreased with the number of consecutive reactions, so that at the seventh hydrolysis reaction the activity recovery was approximately 70% and 90% at 25 °C and 40 °C, respectively. These findings revealed that the

stability of lipases immobilized onto PS/PEG/CR is favored at 40 °C and deactivations by desorption or conformational changes are minimal. Thus, lipases immobilized onto PS/PEG/CR particles are advantageous because the cumulative activity after seven reactions overcomes in approximately 6-fold the activity of free lipase, which cannot be recovered for reuse. Moreover, lipases immobilized onto PS/PEG/CR particles can be stored for 7 days at room temperature, keeping the original catalytic activity. On the other hand, lipases immobilized onto PS/PEG particles ($Q_{\text{lipase}} = 85 \pm 3 \text{ nmol}\cdot\text{mg}^{-1}$) could not be recycled, although the K_M values for this system was the smallest one (Table 2).

Figure 6. Activity recovery determined at 25 °C and 40 °C for lipases immobilized onto PS/PEG/CR particles ($Q_{\text{lipase}} = 105 \pm 5 \text{ nmol}\cdot\text{mg}^{-1}$). Each point is the average of triplicates \pm SD.



3. Experimental Section

3.1. Materials

Styrene (S; Fluka, St. Gallen, Switzerland), potassium persulfate ($\text{K}_2\text{S}_2\text{O}_8$, Merck, Darmstadt, Germany) and poly(ethylene glycol) sorbitan monolaurate (Tween-20, Sigma-Aldrich Co., St. Louis, MO, USA) were used in the emulsion polymerization. Congo red (CR) was provided by Sigma-Aldrich (São Paulo, Brazil). Chemical structures of Tween-20 and CR are schematically shown in the Scheme 1. Lipase from *Candida rugosa* (~60 kDa [42], isoelectric point at pH 4.5 [21], L1754) and *p*-nitrophenyl butyrate, (*p*-NPB, N9876) were provided by Sigma-Aldrich (Brazil). All reagents were used as received. Silicon (Si/SiO₂) wafers (100) with a native silicon oxide layer of approximately 2 nm thick from University Wafers (Boston, MA, USA), cut in a typical dimension of 1 cm² and rinsed in a standard manner [10,30] were used as substrates for ellipsometry.

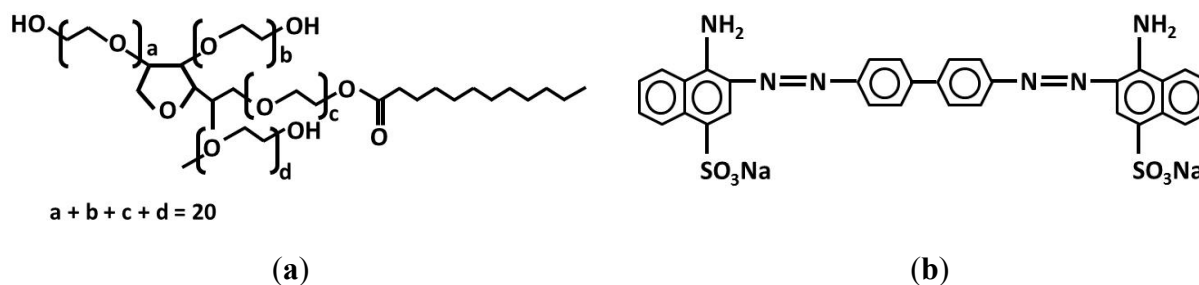
3.2. Methods

3.2.1. Preparation of PS/PEG and PS/PEG/CR Particles

The PS/PEG particles were synthesized following a typical emulsion polymerization recipe, as described elsewhere [16–18]. The polymerization took place in a four neck flask containing 100 mL of Tween-20 solution at $4.8 \times 10^{-5} \text{ mol}\cdot\text{L}^{-1}$, which is close to the critical micelle concentration (c.m.c.).

The system was purged with N_2 during the whole process and the polymerization was carried out under reflux with water and mechanical stirring at 500 rpm. The temperature was set to $(75 \pm 2)^\circ C$, then, 10 mL of styrene were added and the temperature was brought up to $(80 \pm 2)^\circ C$. Afterwards, 1.0 g of $K_2S_2O_8$ (initiator) was added. The synthesis was carried out for 2 h. Then, the system was cooled to room temperature. The dispersion was dialyzed (dialysis membrane 14,000 MW; Viskase Corp., Darien, IL, USA) until ionic conductivity achieved $5 \mu S \cdot cm^{-1}$.

Scheme 1. Representation of chemical structures of (a) Tween-20 and (b) Congo red (CR).



From a previous study [18] one observed that the adsorbed amount of CR (Q_{CR}) onto polymer particles at $(24 \pm 1)^\circ C$ and pH 7 increased with CR concentration up to the onset for the adsorption plateau, at $7.3 \mu mol \cdot L^{-1}$ CR, and Q_{CR} value of $4.73 \pm 0.02 \mu mol \cdot g^{-1}$. Therefore, we used this experimental condition to cover the PS/PEG particles with CR molecules.

3.2.2. Adsorption Isotherms of Lipase onto PS/PEG or PS/PEG/CR Particles

The adsorption isotherms for lipase onto PS/PEG or PS/PEG/CR particles were obtained at $(24 \pm 1)^\circ C$ and pH 7, in the lipase concentration range of $3 \mu mol \cdot L^{-1}$ to $33 \mu mol \cdot L^{-1}$ and constant $N_p = 1.7 \times 10^{10}$ particles mL^{-1} . Lipase and nanoparticles interacted for 24 h under constant rotation at 3 rpm in a home-made vertical carousel. The adsorption time of 24 h was enough to assure equilibrium conditions. Then the dispersions were centrifuged at 12,045 g for 30 min, and their supernatants were separated from the particles. The concentration of free lipase in the supernatants was determined by UV-Vis spectrophotometry at 280 nm in a DU640 spectrophotometer (Beckman-Coulter, Brea, CA, USA) using molar absorptivity $\epsilon = 76365 (L \cdot mol^{-1} \cdot cm^{-1})$ [10]. The medium pH and temperature used for the calibration curve were the same as those used in the adsorption experiments. The concentration of adsorbed lipase onto the particles was calculated as the difference between the initial lipase concentration and the free lipase concentration in the supernatant. The adsorbed amount of lipase (Q_{lipase}) onto polymer particles was calculated dividing the concentration of adsorbed lipase by the mass of PS/PEG or PS/PEG/CR particles in the dispersion at $N_p = 1.7 \times 10^{10}$ particles mL^{-1} . Thus the unit corresponding to Q_{lipase} is $\mu mol \cdot g^{-1}$. The particle mean diameter (D), polydispersity (P) and mean ζ -potential were determined after each adsorption experiment, centrifugation, complete supernatant removal for the quantification of free lipase and re-dispersion in KCl $10 mmol \cdot L^{-1}$, see details below.

3.2.3. Characterization of PS/PEG and PS/PEG/CR Particles before and after Lipase Adsorption

Particle size (zeta-average diameter, D), size distribution, polydispersity (P) and zeta-potential (ζ) values were determined with the ZetaPlus-ZetaPotential Analyzer (Brookhaven Instruments Corporation, Holtsville, NY, USA), which was equipped with a 677 nm laser and dynamic light-scattering (DLS) photon correlation spectroscopy at 90° for particle sizing. Mean diameter values were obtained by fitting data to log-normal size distributions which do not discriminate between one, two, or more different populations and considers always all scattering particles as belonging to one single Gaussian population. On the other hand, for the size distribution and P data, fitting was performed by the apparatus software using the non-negatively constrained least squares algorithm, which is a model independent technique allowing to achieve multimodal distributions [43]. Zeta-potential (ζ) was determined from electrophoretic mobility (μ) in 10 mmol·L⁻¹ KCl and the Smoluchowski equation $\zeta = \mu\eta/\epsilon$, where η is the medium viscosity and ϵ the medium dielectric constant.

The mean particle number density (N_p) was calculated considering the particle mean diameter calculated by DLS and the solid content, as described elsewhere [44].

In order to gain more insight about the adsorption behavior of lipase onto PS/PEG or PS/PEG/CR particles, the particles were characterized before and after lipase adsorption with N_p on the order of 10⁸ particles mL⁻¹. After lipase adsorption the dispersions were centrifuged, the supernatant was replaced by pure water and the particles were re-dispersed. This procedure was repeated once more and then the size distribution and zeta potential values were analyzed.

Scanning electron microscopy (SEM) analyses were performed to determine the morphology of dried particles using SEM-FEG JEOL 7401F equipment (Jeol, Tokyo, Japan). The stock dispersions were diluted 1,000 times in Milli-Q water; then droplets were deposited onto clean Si wafers. The water evaporated slowly at room temperature. The dried dispersions were coated with a 3 nm gold layer.

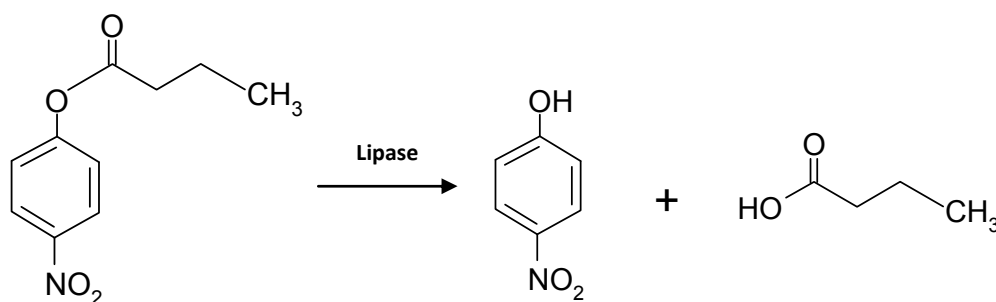
3.2.4. Desorption Experiments

Lipase covered PS/PEG or PS/PEG/CR particles were submitted to desorption tests. After lipase adsorption and centrifugation the supernatant was removed from the tubes and initial volume was completed with pure solvent (distilled water). The dispersions were kept for 24 h under constant rotation at 3 rpm. The dispersions were then centrifuged at 12,045 g for 30 min and the absorbance of the supernatant was measured in order to determine the concentration of desorbed lipase. The desorbed amount didn't change significantly after 24 h in contact with pure solvent.

3.2.5. Catalytic Activity of Immobilized Lipase and Free Lipase

The activity of free lipase and lipase immobilized onto PS/PEG or PS/PEG/CR particles was determined by measuring the formation of *para*-nitrophenol (*p*-NP), as a result of enzymatic hydrolysis of (*p*-NPB), as indicated in Scheme 2.

Scheme 2. Representation of *p*-NPB hydrolysis catalyzed by lipase, yielding butyric acid and (*p*-NP).



The formation of *p*-NP was monitored by means of a Beckmann Coulter DU 640 UV-VIS spectrophotometer operating at a fixed wavelength of 400 nm and (24 ± 1) °C. The concentration of *p*-NP formed was calculated using molar extinction coefficient $\epsilon = 13800 \text{ L mol}^{-1} \text{ cm}^{-1}$ [45]. First, 25 μL of *p*-NPB (M 209.2 g/mol, density 1.19 g/cm³) was dissolved in 5.0 mL of isopropanol. After that, *p*-NPB solution was added to 45 mL of Tris-HCl 0.050 mol/L buffer (pH 7.5), yielding the concentration of stock solution of *p*-NPB as $2.8 \times 10^{-3} \text{ mol/L}$. The kinetic parameters were determined in the *p*-NPB concentration range from $0.3 \times 10^{-3} \text{ mol/L}$ to $2.8 \times 10^{-3} \text{ mol/L}$ at 25 °C. The volume and concentration of each reagent mixed in the spectrophotometric cell were the following: 20 μL of dispersions containing lipase immobilized onto PS/PEG ($Q_{\text{lipase}} = 85 \pm 3 \text{ nmol}\cdot\text{mg}^{-1}$) or PS/PEG/CR ($Q_{\text{lipase}} = 105 \pm 5 \text{ nmol}\cdot\text{mg}^{-1}$), a given volume of stock solution of *p*-NPB to achieve the desired concentration and 50 mM Tris-HCl buffer to complete the total volume of 1.0 mL. In order to compare the catalytic efficiency between free and immobilized lipase, the concentration of free lipase was set as $18 \mu\text{mol}\cdot\text{L}^{-1}$ because it corresponds to the highest Q_{lipase} onto PS/PEG or PS/PEG/CR particles. Thus, the final concentration of free lipase or lipase immobilized onto polymeric particles in the spectrophotometric cell was $0.4 \mu\text{mol}\cdot\text{L}^{-1}$. Control experiments were performed, where bare PS/PEG or bare PS/PEG/CR particles were added to the enzymatic reaction in the absence of lipase and the formation of *p*-NP was monitored by UV-Vis spectrophotometry ($\lambda_{\text{max}} = 400 \text{ nm}$) as a function of time. In a similar way, the activity of lipase immobilized onto PS/PEG or PS/PEG/CR particles was determined at 25 °C and 40 °C after seven consecutive recycles or after storing during seven days in the laboratory environment.

Thermal stability of free and immobilized lipases was investigated by monitoring the concentration of *p*-NP formed during 20 min in the temperature range between 25 °C and 60 °C. The volume and concentration of each reagent mixed in the spectrophotometric cell were the following: 20 μL of dispersions containing lipase immobilized onto PS/PEG ($Q_{\text{lipase}} = 85 \pm 3 \text{ nmol}\cdot\text{mg}^{-1}$) or PS/PEG/CR ($Q_{\text{lipase}} = 105 \pm 5 \text{ nmol}\cdot\text{mg}^{-1}$), 250 μL of stock solution of *p*-NPB to achieve $0.7 \times 10^{-3} \text{ mol}\cdot\text{L}^{-1}$ and 50 mM Tris-HCl buffer to complete the total volume of 1.0 mL.

3.2.6. Evaluation of Bioconjugation Effects

Circular dichroism (CD) measurements were performed on a Jasco J-720 spectropolarimeter (Jasco, Easton, MD, USA), in the wavelength range of 190 nm to 260 nm, at (24 ± 1) °C, using a 0.5 cm quartz cell. All CD spectra were collected at pH 7 using scan speed of $50 \text{ nm}\cdot\text{min}^{-1}$, time constant of 0.5 s and bandwidth of 1 nm. Eight scans were accumulated for each sample. The samples for CD were

prepared with lipase solutions at concentration range of $3 \mu\text{mol}\cdot\text{L}^{-1}$ to $33 \mu\text{mol}\cdot\text{L}^{-1}$ in the absence and in the presence of CR at constant concentration of $8.0 \mu\text{mol}\cdot\text{L}^{-1}$. More diluted lipase solutions yielded no CD signal.

Changes in the electronic spectra of CR in the visible range were monitored by increasing addition of lipase. The CR concentration was kept constant at $8.0 \mu\text{mol}\cdot\text{L}^{-1}$, while the lipase concentration increased from $3 \mu\text{mol}\cdot\text{L}^{-1}$ to $33 \mu\text{mol}\cdot\text{L}^{-1}$. Bioconjugation between CR molecules and *p*-NPB was evaluated by monitoring the changes in the electronic spectra of CR at $8.0 \mu\text{mol}\cdot\text{L}^{-1}$ in the presence of *p*-NPB in the concentration range of $0.3 \times 10^{-3} \text{ mol}\cdot\text{L}^{-1}$ to $2.8 \times 10^{-3} \text{ mol}\cdot\text{L}^{-1}$.

3.2.7. Ellipsometry

The mean thickness of the adsorbed lipase layers was determined by ellipsometry using a vertical computer-controlled DRE-EL02 ellipsometer (Ratzeburg, Germany) with an angle of incidence ϕ of 70.0° and wavelength λ of 632.8 nm He–Ne laser. Using the fundamental ellipsometric equation [29]:

$$e^{i\Delta} \tan \psi = (R_p/R_s) = f(n_k, d_k, \lambda, \phi) \quad (1)$$

where R_p and R_s are the overall reflection coefficients for parallel and perpendicular waves, respectively. The mean thickness d_k and refractive index n_k can be calculated from variation of the ellipsometric angles Δ and Ψ using iterative calculations and a multilayer model composed by the substrate, the unknown layer, and surrounding medium. The thickness of the SiO_2 layer was determined in air, considering the indices of refraction for Si as $n_{\text{Si}} = (3.88 - i0.018)$, $n_{\text{air}} = 1.00$ and $n_{\text{SiO}_2} = 1.462$ and “infinite” thickness for the Si and air layers. The mean thickness obtained for SiO_2 was (2.0 ± 0.1) nm. For the CR adsorbed layer onto Si/ SiO_2 , n_{CR} was 1.59 and $d_{\text{CR}} = (1.4 \pm 0.2)$ nm. After that the thickness values for the lipase layer, d_{lipase} , adsorbed onto Si/ SiO_2 or Si/ SiO_2 /CR were calculated using refractive index $n = 1.52$ [10]. The d_{lipase} values were calculated in the air just after the equilibrium adsorption.

4. Conclusions

Lipases adsorbed physically onto polymeric nanoparticles decorated either with PEG or with CR. The affinity of *p*-NPB for lipases immobilized onto PS/PEG particles was larger than that for free lipases or for lipases immobilized onto PS/PEG/CR particles. On the other hand, the hydrolysis rate observed for lipases immobilized onto PS/PEG/PS particles was larger than those observed for free lipases or for lipases onto PS/PEG particles. The main reasons for this are bioconjugation effects, which favor: (i) the interactions between the hydrophobic moieties of CR and the lid, maintaining the open state conformation and (ii) hydrated environment close to the active site to enable the hydrolysis reaction. Thus, although the affinity between lipase immobilized onto PS/PEG and the substrate was high, the open state conformation was unfavored. PS/PEG/CR particles are easily prepared and cheap (\sim US\$ 1.00 per liter of dispersions with $N_p = 1.7 \times 10^{14}$ particles L^{-1}). For practical purposes, the immobilization of lipases on them is advantageous because they can be used efficiently as catalysts, retaining their catalytic properties after seven repeated cycles, and can be stored in the laboratory environment over seven days retaining activity at a high level.

Acknowledgments

The study was supported by Conselho Nacional de Pesquisa e Desenvolvimento (Grants # 305178/2013, 470105/2010-0), Fundação de Amparo à Pesquisa do Estado de São Paulo (Grant # 2011/00046-5) and Rede Nanobiotec CAPES.

Author Contributions

R.A.S. performed the experiments and participated in the discussion of results, A.M.C.R. participated in the discussion of results and D.F.S.P. designed the experiments and wrote the manuscript.

Conflicts of Interest

The authors declare no conflict of interest.

References

1. Di Cosimo, R.; McAuliffe, J.; Poulou, A.J.; Bohlmann, G. Industrial use of immobilized enzymes. *Chem. Soc. Rev.* **2013**, *42*, 6437–6474.
2. Kapoor, M.; Gupta, M.N. Lipase promiscuity and its biochemical applications. *Proc. Biochem.* **2012**, *47*, 555–569.
3. Schrag, J.D.; Cygler, M. Lipases and α/β hydrolase fold. *Methods Enzymol.* **1997**, *284*, 85–107.
4. Carrasco-Lopez, C.; Godoy, C.; de las Rivas, B.; Fernandez-Lorente, G.; Palomo, J.M.; Guisan, J.M. Activation of bacterial thermoalkalophilic lipases is spurred by dramatic structural rearrangements. *J. Biol. Chem.* **2009**, *284*, 4365–4372.
5. Hanefeld, U.; Gardossi, L.; Magner, E. Understanding enzyme immobilisation. *Chem. Soc. Rev.* **2009**, *38*, 453–468.
6. Cicolatti, E.P.; Silva, M.J.A.; Klein, M.; Feddern, V.; Feltes, M.M.C.; Oliveira, J.V.; Ninow, J.L.; Oliveira, D. Current status and trends in enzymatic nanoimmobilization. *J. Mol. Catal. B Enzym.* **2014**, *99*, 56–67.
7. Rodrigues, R.C.; Ortiz, C.; Berenguer-Murcia, A.; Torres, R.; Fernández-Lafuente, R. Modifying enzyme activity and selectivity by immobilization. *Chem. Soc. Rev.* **2013**, *42*, 6290–6307.
8. Mendes, A.A.; Oliveira, P.C.; de Castro, H.F. Properties and biotechnological applications of porcine pancreatic lipase. *J. Mol. Catal. B Enzym.* **2012**, *78*, 119–134.
9. Sheldon, R.A.; van Pelt, S. Enzyme immobilisation in biocatalysis: Why, what and how. *Chem. Soc. Rev.* **2013**, *42*, 6223–6235.
10. Kosaka, P.M.; Kawano, Y.; El Seoud, O.A.; Petri, D.F.S. Catalytic activity of lipase immobilized onto ultrathin films of cellulose esters. *Langmuir* **2007**, *23*, 12167–12173.
11. Chen, Y.Z.; Yang, C.T.; Ching, C.B.; Xu, R. Immobilization of lipases on hydrophobized zirconia nanoparticles: Highly enantioselective and reusable biocatalysts. *Langmuir* **2008**, *24*, 8877–8884.
12. Boscolo, B.; Trotta, F.; Ghibaudi, E. High catalytic performances of *Pseudomonas fluorescens* lipase adsorbed on a new type of cyclodextrin-based nanosponges. *J. Mol. Catal. B Enzym.* **2010**, *62*, 155–161.

13. Bellusci, M.; Francolini, I.; Martinelli, A.; D'Ilario, L.; Piozzi, A. Lipase immobilization on differently functionalized vinyl-based amphiphilic polymers: Influence of phase segregation on the enzyme hydrolytic activity. *Biomacromolecules* **2012**, *13*, 805–813.
14. Li, L.; Feng, W.; Pan, K. Immobilization of lipase on amino-cyclodextrin functionalized carbon nanotubes for enzymatic catalysis at the ionic liquid–organic solvent interface. *Colloids Surf. B* **2013**, *102*, 124–129.
15. Peng, Y.; Zhu-Ping, H.; Yong-Juan, X.; Peng-Cheng, H.; Ji-Jun, T. Effect of support surface chemistry on lipase adsorption and activity. *J. Mol. Catal. B Enzym.* **2013**, *94*, 69–76.
16. Bonfá, A.; Saito, R.S.N.; França, R.F.O.; Fonseca, B.A.L.; Petri, D.F.S. Poly(ethylene glycol) decorated poly(methylmethacrylate) nanoparticles for protein adsorption. *Mater. Sci. Eng. C* **2011**, *31*, 562–566.
17. Blachechen, L.S.; Silva, J.O.; Barbosa, L.R.S.; Itri, R.; Petri, D.S.F. Hofmeister effects on the colloidal stability of poly(ethylene glycol)-decorated nanoparticles. *Colloid Polym. Sci.* **2012**, *290*, 1537–1546.
18. Silva, R.A.; Carmona-Ribeiro, A.M.; Petri, D.F.S. Enzymatic activity of cholesterol oxidase immobilized onto polymer nanoparticles mediated by Congo red. *Colloids Surf. B* **2013**, *110*, 347–355.
19. Alkschbirs, M.I.; Bizotto, V.C.; Oliveira, M.G.; Sabadini, E. Effects of congo red on the drag reduction properties of Poly(ethylene oxide) in aqueous solution based on drop impact images. *Langmuir* **2004**, *20*, 11315–11320.
20. Cooper, T.M.; Campbell, A.L.; Crane, R.L. Formation of polypeptide-dye multilayers by an electrostatic self-assembly technique. *Langmuir* **1995**, *11*, 2713–2718.
21. Sharma, R.; Chistib, Y.; Banerjee, U.C. Production, purification, characterization, and applications of lipases. *Biotechnol. Adv.* **2001**, *19*, 627–662.
22. Pancera, S.M.; Itri, R.; Petri, D.F.S. Small-angle X-ray scattering on solutions of carboxymethylcellulose and bovine serum albumin. *Macromol. Biosci.* **2005**, *5*, 331–336.
23. Silva, R.A.; Urzúa, M.D.; Petri, D.F.S.; Dubin, P.L. Protein adsorption onto polyelectrolyte layers: Effects of protein hydrophobicity and charge anisotropy. *Langmuir* **2010**, *26*, 14032–14038.
24. Palomo, J.M.; Fuentes, M.; Fernández-Lorente, G.; Mateo, C.; Guisan, J.M.; Fernández-Lafuente, R. General trend of lipase to self-assemble giving bimolecular aggregates greatly modifies the enzyme functionality. *Biomacromolecules* **2003**, *4*, 1–6.
25. Fernández-Lorente, G.; Palomo, J.M.; Fuentes, M.; Mateo, C.; Guisán, J.M.; Fernández-Lafuente, R. Self-assembly of *Pseudomonas fluorescens* lipase into bimolecular aggregates dramatically affects functional properties. *Biotechnol. Bioeng.* **2003**, *82*, 232–237.
26. Palomo, J.M.; Ortiz, C.; Fuentes, M.; Fernandez-Lorente, G.; Guisan, J.M.; Fernandez-Lafuente, R. Use of immobilized lipases for lipase purification via specific lipase-lipase interactions. *J. Chromatogr. A* **2004**, *1038*, 267–273.
27. Palomo, J.M.; Ortiz, C.; Fernández-Lorente, G.; Fuentes, M.; Guisán, J.M.; Fernández-Lafuente, R. Lipase-lipase interactions as a new tool to immobilize and modulate the lipase properties. *Enzyme Microb. Technol.* **2005**, *36*, 447–454.

28. Wilson, L.; Palomo, J.M.; Fernández-Lorente, G.; Illanes, A.; Guisán, J.M.; Fernández-Lafuente, R. Effect of lipase-lipase interactions in the activity, stability and specificity of a lipase from *Alcaligenes sp.* *Enzyme Microb. Technol.* **2006**, *39*, 259–264.
29. Azzam, R.M.A.; Bashara, N.M. *Ellipsometry and Polarized Light*; North Holland Personal Library: Amsterdam, The Netherlands, 1996.
30. Pancera, S.M.; Gliemann, H.; Schimmel, T.; Petri, D.F.S. Effect of pH on the adsorption and activity of creatine phosphokinase. *J. Phys. Chem. B* **2006**, *110*, 2674–2680.
31. Peter, G.H.; van Aalten, D.M.F.; Edfolm, O.; Toxvaerd, S.; Bywater, R. Dynamics of Proteins in Different Solvent Systems: Analysis of Essential Motion in Lipases. *Biophys. J.* **1996**, *71*, 2245–2255.
32. Yu, J.; Wei, X.; Zhang, L.; Fang, X.; Yang, T.; Huang, F.; Liang, W. Polyethylene glycol (PEG)-mediated conformational alteration of α -chymotrypsin prevents inactivation of insulin by stabilizing active intermediates. *Mol. Pharm.* **2014**, doi:10.1021/mp500001n.
33. Pancera, S.M.; Petri, D.F.S.; Itri, R. The effect of poly(ethylene glycol) on the activity, structural conformation and stability of yeast hexokinase. *Prog. Colloid Polym. Sci.* **2004**, *128*, 178–183.
34. Pancera, S.M.; da Silva, L.H.M.; Loh, W.; Itri, R.; Pessoa, A., Jr.; Petri, D.F.S. The effect of Poly(ethylene glycol) on the activity and structure of glucose-6-phosphate dehydrogenase in solution. *Colloids Surf. B* **2002**, *26*, 291–300.
35. Polizelli, P.P.; Tiera, M.J.; Bonilla-Rodriguez, G.O. Effect of surfactants and polyethylene glycol on the activity and stability of a lipase from oilseeds of *Pachira aquatica*. *J. Am. Oil Chem. Soc.* **2008**, *85*, 749–753.
36. Bayramoglu, G.; Hazer, B.; Altıntas, B.; Arica, M.Y. Covalent immobilization of lipase onto amine functionalized polypropylene membrane and its application in green apple flavor (ethyl valerate) synthesis. *Proc. Biochem.* **2011**, *46*, 372–378.
37. Hatzinikolaou, D.G.; Kourentzi, E.; Stamatis, H.; Christakopoulos, P.; Kolisis, F.N.; Kekos, D.; Macris, B.J. A novel lipolytic activity of *Rhodotorula glutinis* cells: Production, partial characterization and application in the synthesis of esters. *J. Biosci. Bioeng.* **1999**, *88*, 53–56.
38. Mateo, C.; Palomo, J.M.; Fernandez-Lorente, G.; Guisan, J.M.; Fernandez-Lafuente, R. Improvement of enzyme activity, stability and selectivity via immobilization techniques. *Enzym. Microb. Technol.* **2007**, *40*, 1451–1463.
39. Dodson, G.G.; Lawson, D.M.; Winkler, F.K. Structural and evolutionary relationships in lipase mechanism and activation. *Faraday Discuss.* **1992**, *93*, 95–105.
40. Fabian, J.; Hartmann, H. *Light Absorption of Organic Colorants*; Springer-Verlag: Berlin, Germany, 1980.
41. Pereira, E.B.; Zanin, G.M.; Castro, H.F. Immobilization and catalytic properties of lipase on chitosan for hydrolysis and esterification reactions. *J. Braz. Chem. Eng.* **2003**, *20*, 343–355.
42. Benjamin, S.; Pandey, A. Isolation and characterization of three distinct forms of lipases from *Candida rugosa* produced in solid state fermentation. *Braz. Arch. Biol. Technol.* **2000**, *43*, 453–460.
43. Grabowski, E.F.; Morrison, I.D. Particle size distribution from analysis of quasielastic light scattering data. In *Measurements of Suspended Particles by Quasi-Elastic Light Scattering*; Dahneke, B.E., Ed.; Wiley: New York, NY, USA, 1983; pp. 199–236.

44. Castro, L.B.R.; Soares, K.V.; Naves, A.F.; Carmona-Ribeiro, A.M.; Petri, D.F.S. Synthesis of stable polystyrene and poly(methyl methacrylate) particles in the presence of carboxymethyl Cellulose. *Ind. Eng. Chem. Res.* **2004**, *43*, 7774–7779.
45. Iacazio, G.; Périssol, C.; Faure, B. A new tannase substrate for spectrophotometric assay. *J. Microbiol. Methods* **2000**, *42*, 209–214.

Sample Availability: Colloidal dispersions of PS/PEG, PS/PEG/CR and PS/PEG/CR coated with lipases are available from the authors.

© 2014 by the authors; licensee MDPI, Basel, Switzerland. This article is an open access article distributed under the terms and conditions of the Creative Commons Attribution license (<http://creativecommons.org/licenses/by/3.0/>).